ditions. The solvent Me_2SO-d_6 was selected for variable-temperature studies to determine activation parameters since this solvent has a higher boiling point.

Enzyme Assays. Frozen rat eyes were purchased from Charles River Breeding Labs, Inc., Wilmington, MA. The lenses were dissected from the partially thawed eyes and kept frozen until used for enzyme isolation. Crude enzyme supernatant was prepared by homogenizing 100 lenses in distilled water (20 mL) and then centrifuging the crude homogenate at 10000 rpm for 15 min while maintaining an ambient temperature of 5 °C. The supernatant was then isolated and ammonium sulfate was added to achieve 40% saturation, and this solution centrifuged at 10000 rpm for 15 min at 5 °C.

Aldose reductase activity of the freshly prepared 40% ammonium sulfate supernatant was assayed spectrophotometrically at 30 °C by measuring the decrease in NADPH concentration at 340 nm with a Shimadzu UV-160 spectrophotometer equipped with a thermocontrolled multicell positioner. The control reaction mixture contained 0.1 M phosphate buffer, pH 6.2; 0.104 mM NADPH and 10 mM DL-glyceraldehyde and 0.2 mL of the enzyme supernatant in a total volume of 2.0 mL. A reference blank containing all of the above reagents except the substrate glyceraldehyde was used to correct for oxidation of NADPH not associated with reduction of the substrate. The reactions were initiated by addition of glyceraldehyde and were monitored for 3 min after a 45-s incubation period. Enzyme activity was adjusted by dilution of the supernatant with distilled water so that 0.2 mL of supernatant gave an average reaction rate for control reactions of 0.0120 ± 0.002 absorbance units per minute. The inhibitory activity of the *N*-benzoyl amino acids was determined by including 0.2 mL of an aqueous solution of the inhibitor at the desired concentrations in the reaction mixture. For IC_{50} determinations, each inhibitor was tested at no fewer than six different concentrations with a minimum of two determinations at each concentration. The percent inhibition for each inhibitor was calculated at all concentrations by comparing the rate of reactions containing inhibitor to that of control reactions with no inhibitor. Inhibitor IC_{50} value were then obtained by least-squares analyses of the linear portion of log dose–response curves using the LINEFIT program of Barlow.[10]

Kinetic Studies. Kinetic analyses (Figure 1) with **5f** were conducted using a minimum of four concentrations (0.5, 1.0, 5.0, and 10.0 μM) of the inhibitor. For substrate kinetics, the concentrations of DL-glyceraldehyde ranged from 1.25 to 0.078 mM, and the concentration of cofactor was held constant at 0.104 mM. For cofactor kinetics, the concentrations of NADPH were varied from 3.25 to 105 μM and the substrate concentration held constant at 10 mM. The nature of inhibition produced by each concentration of inhibitor was determined by analysis of double reciprocal plots of enzyme velocity versus DL-glyceraldehyde or NADPH concentration as generated by least-squares fit of the data using the program of Barlow.[10]

Acknowledgment. We express our appreciation to Paula Monk and Robert B. Knowles for their assistance in the synthesis and biochemical evaluation of the inhibitors. This study was supported by a gift from the W. W. Walker, Jr., Endowment.

Registry No. **3a**, 495-69-2; **3b**, 75446-60-5; **3c**, 69826-63-7; **3d**, 133604-60-1; **3e**, 133604-61-2; **3f**, 133604-62-3; **3g**, 133604-63-4; **4a**, 2568-34-5; 4b, 133604-64-5; **4c**, 133604-65-6; **4d**, 133604-66-7; **4e**, 133604-67-8; **4f**, 35876-37-0; **4g**, 133604-68-9; **4h**, 133604-69-0; 4i, 133604-70-3; **5a**, 119656-49-4; **5b**, 133604-71-4; **5c**, 35876-73-4; **5d**, 133604-72-5; 5e, 2995-56-4; **5f**, 35876-34-7; **5g**, 119656-55-2; **5h**, 133604-73-6; **5i**, 133604-74-7; ALR2, 9028-31-3; H-Gly-OH, 56-40-6; H-Sar-OH, 107-97-1; PhCOCl, 98-88-4; 4-MeC_6H_4COCl, 874-60-2; 4-$MeOC_6H_4COCl$, 100-07-2; 4-FC_6H_4COCl, 403-43-0; 4-$O_2NC_6H_4COCl$, 122-04-3; 4-$O_2NC_6H_4CO$-Gly-OH, 2645-07-0; 4-$H_2NC_6H_4CO$-Gly-OH, 61-78-9; Ph-Gly-OH, 103-01-5; 1-naphthylcarbonyl chloride, 879-18-5; 2-naphthylcarbonyl chloride, 2243-83-6.

Synthesis and in Vivo Photodynamic Activity of Some Bacteriochlorin Derivatives against Bladder Tumors in Rodents

Alan R. Morgan,*,† Dimitris Skalkos,† Greta M. Garbo,† Rick W. Keck,‡ and Steven H. Selman‡

Departments of Chemistry and Biological and Medicinal Chemistry, University of Toledo, Toledo, Ohio 43606, and Department of Surgery, Medical College of Ohio, CS#10008, Toledo, Ohio 43699. *Received November 30, 1990*

Bacteriochlorins have been suggested as potential photosensitizers for use in photodynamic therapy. We have shown that bacteriochlorin-like macrocycles can be generated through cyclization of either 5,10- or 5,15-bis[(ethoxycarbonyl)vinyl]porphyrins; however, the resulting products are rapidly decomposed on exposure to air. More stable systems can be generated by Diels–Alder reactions between dienophiles such as dimethyl acetylenedicarboxylate or tetracyanoethylene, and vinylporphyrinones. Although spectroscopic properties of these latter products resemble those of porphyrinones rather than bacteriochlorins, in vivo studies using the *N*-[4-(5-nitro-2-furyl)-2-thiazolyl]-formamide-induced rat bladder tumor (AY-27) transplanted into Fisher CDF (F344)/CrlBr rats demonstrated a powerful photodynamic response.

Introduction

The bacteriochlorins (A; Figure 1) are a series of tetrapyrrolic macrocycles that differ from porphyrins (B; Figure 1) only in the reduced state of two opposite pyrrole rings. This difference is suffice to alter dramatically the electromagnetic spectrum of the molecule, with the longer absorbing (Q) band of the porphyrin near 630 nm and the corresponding absorption of the tetrahydro species red-shifted by some 150 nm.[1] Bacteriochlorins have therefore been proposed as potentially useful candidates for use in photodynamic therapy where strong absorptions in the visible spectrum can be used to photoactive dyes previously located in target (neoplastic) tissues.[2] Ensuing energy transfer or electron transfer can then generate cytotoxic species in situ that ultimately lead to tumor necrosis.[3]

Although bacteriochlorophylls, naturally occurring bacteriochlorins, have been shown to photosensitize cells in vitro[4] and have also shown photodynamic activity in

* Author to whom correspondence should be addressed.
† University of Toledo.
‡ Medical College of Ohio.

(1) Smith, K. M. In *Heterocyclic Chemistry*; Katritzky, A. R., Rees, C. W., Eds.; Pergamon Press: New York, 1984; Vol. 4, p 385.
(2) Bonnett, R.; Nizhnik, A. N.; Berenbaum, M. C. *J. Chem. Soc., Chem. Commun.* **1989**, 1822.
(3) Girotti, A. W. *Photochem. Photobiol.* **1983**, *38*, 745.
(4) Beems, E. M.; Dubbelman, T. M. A. R.; Lugtenburg, I.; Van Best, J. A.; Smeets, M. F. M. A.; Boegheim, J. P. S. *Photochem. Photobiol.* **1987**, *46*, 639.

0022-2623/91/1834-2126$02.50/0

Scheme I. Synthesis of Bisacrylates **6** and **7**[a]

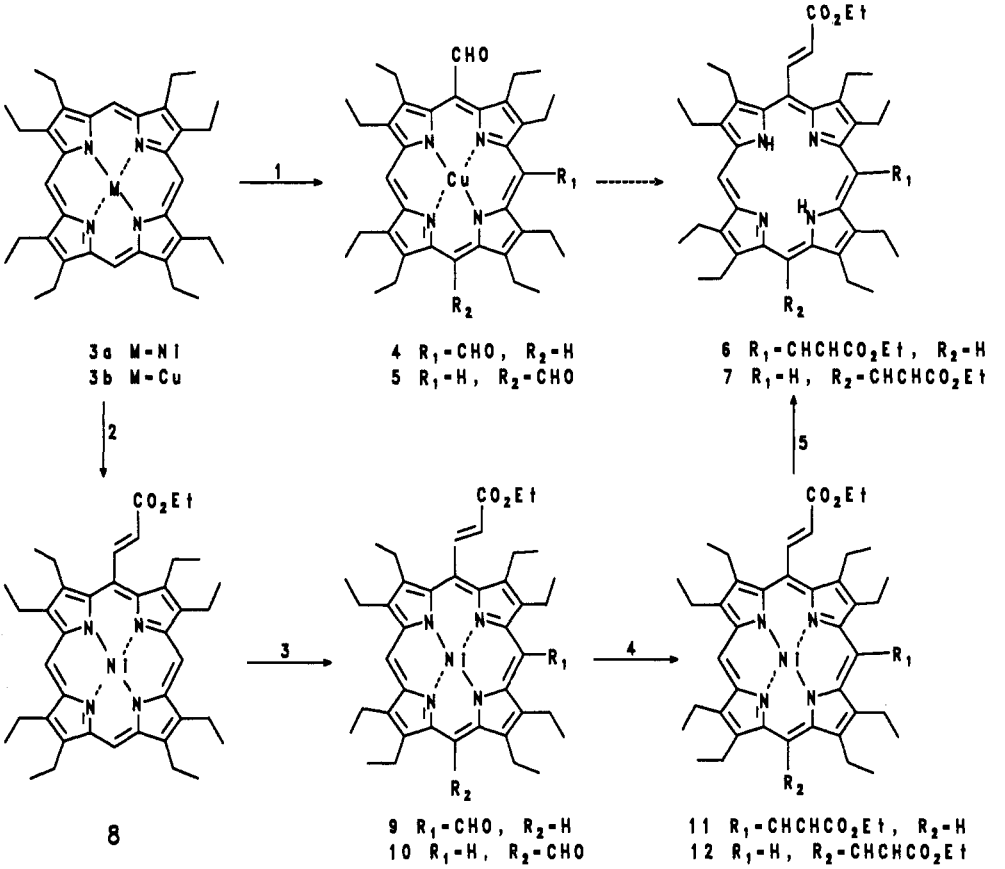

[a] (1) $POCl_3$/DMF, NaOAc; (2) $POCl_3$/DMF, NaOAc; $Ph_3P{=}CHCO_2Et$/xylene; (3) $POCl_3$/DMF, NaOAc; (4) $Ph_3P{=}CHCO_2Et$/xylene; (5) H_2SO_4, $NaHCO_3$.

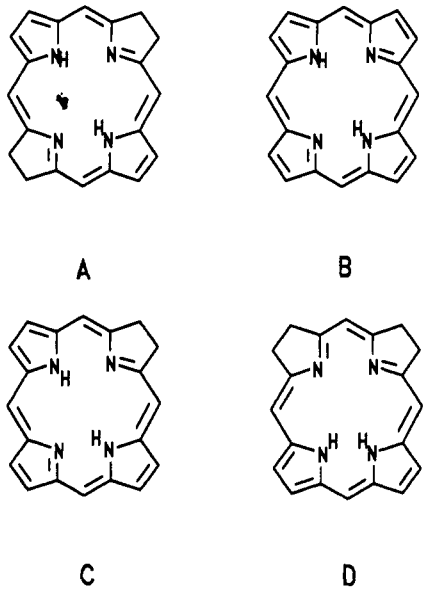

Figure 1. Tetrapyrrolic macrocycles: A = bacteriochlorin; B = porphyrin; C = Chlorin; D = isobacteriochlorin.

vivo,[5] the progress made in the study of bacteriochlorins for PDT has been hampered by the sensitivity of the macrocycle to oxygen, which results in rapid oxidation to the chlorin state.[5,6] Chlorins (dihydroporphyrins) (C; Figure 1) are characterized by Q bands absorbing at ca. 660 nm; thus the spectroscopic properties of the bacteriochlorin are lost.[1] If, as is usually the case, a laser is used to excite the bacteriochlorin in vivo, oxidation may result in formation of a new chromophor absorbing outside of the laser window, thus reducing the photodynamic efficiency.

We describe here the preparation of two novel bacteriochlorin systems and assess their potential for use in photodynamic therapy by a study of their photodynamic activity against the *N*-[4-(5-nitro-2-furyl)-2-thiazolyl]-formamide (FANFT)-induced urothelial cell carcinoma transplanted into rats—a model we have previously used for the investigation of other classes of sensitizers as photodynamic agents.[7]

Synthesis of Bacteriochlorins. From *meso*-[β-(Ethoxycarbonyl)vinyl]porphyrins (Purpurin Route). We have previously described the cyclization of *meso*-[β-(ethoxycarbonyl)vinyl]porphyrins to generate the corresponding purpurins (e.g. **1** → **2**; Figure 2).[8] Since these macrocycles are at the oxidation state of a chlorin (and indeed, generate visible spectra identical with those of chlorins on hydrogenation of the isocyclic ring), it appeared reasonable to expect macrocycles bearing two iso-

(5) Henderson, B. W.; Potter, W. R.; Sumlin, A. B.; Owczarczak, F. S.; Doughterty, T. J. *Photodynamic Therapy: Mechanisms II. SPIE Vol. 1203*; Dougherty, T. J., Ed.; SPIE: Bellingham, WA, 1990; p 211.

(6) (a) Smith, J. R. L.; Calvin, M. *J. Am. Chem. Soc.* **1966**, *88*, 4500. (b) Scheer, H.; Svec; W. A.; Cope, B. T.; Studier, M. H.; Scott, R. G.; Katz, J. J. *J. Am. Chem. Soc.* **1974**, *96*, 3714.

(7) (a) Morgan, A. R.; Garbo, G. M.; Birnbaum, M. K.; Keck, R. W.; Chaudhuri, K.; Selman, S. H. *Cancer Res.* **1987**, *47*, 496. (b) Morgan, A. R.; Garbo, G. M.; Keck, R. W.; Miller, R. A.; Selman, S. H.; Skalkos, D. *J. Med. Chem.* **1990**, *33*, 1258. (c) Morgan, A. R.; Garbo, G. M.; Keck, R. W.; Skalkos, D.; Selman, S. H. *Photochem. Photobiol. B. Biol.* **1990**, *6*, 133.

(8) Morgan, A. R.; Tertel, N. C. *J. Org. Chem.* **1986**, *51*, 1347.

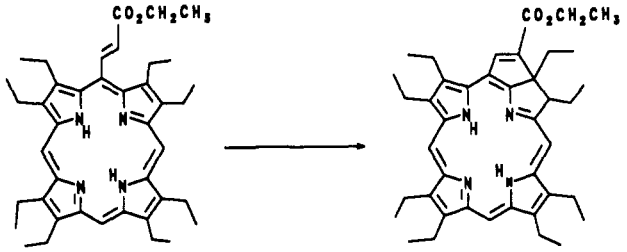

1 2

Figure 2. Synthesis of octaethylpurpurin **2**.

cyclic rings (attached to opposite pyrroles) to exhibit spectroscopic properties similar to those of bacteriochlorins. The question therefore became: could cyclization of both *meso*-β-(ethoxycarbonyl)vinyl substituents of a 5,10- or 5,15-disubstituted porphyrin be effected and, if so, would cyclization occur at opposite or adjacent pyrrole rings (forming either bacteriochlorins [A; Figure 1] or isobacteriochlorins [D; Figure 1], respectively).

We began the synthesis with an attempt to prepare copper 5,10- and 5,15-diformyloctaethylporphyrins **4** and **5** as precursors for the required bisacrylates (**6** and **7** Scheme I). Although nickel octaethylporphyrin (**3a**) has been shown to undergo monoformylation only,[9] it has been reported that the copper derivative **3b**, when formylated using Vilsmeir conditions, gives a modest yield (23%) of the 5,10- and 5,15-diformyl isomers (**4** and **5**).[10] Unfortunately, this reaction gave even more modest yields in our hands and we abandoned this approach in favor of an alternative route. Thus, nickel 5-[β-(ethoxycarbonyl)-vinyl]octaethylporphyrin (**8**) was prepared as previously described[8] and subjected to Vilsmeir formylation to give nickel 5-[β-(ethoxycarbonyl)vinyl]-10-formyloctaethylporphyrin (**9**) and nickel 5-[β-(ethoxycarbonyl)vinyl]-15-formyloctaethylporphyrin (**10**) in good yield (45% ratio 2:1). Each isomer was separated by silica gel chromatography and identified by ^1H NMR spectroscopy, where the component having one meso resonance (δ 9.07 ppm; both meso protons equivalent) was assigned the 5,15-substituted isomer **10** and the component having two meso resonances (δ 9.01, 9.07 ppm; nonequivalent meso protons) was assigned as the 5,10-substituted isomer **9**. We ascribe the ease of formylation of the nickel 5-[β-(ethoxycarbonyl)-vinyl]porphyrin (**8**) and the lack of formylation of the corresponding 5-formylporphyrin to a twisting of the larger acrylate substituent from planarity. This would be expected to result in increased nucleophilicity at the remaining meso positions and hence an increase in reactivity to electrophilic reagents.

Reaction of each isomer (**9**, **10**) with (carbethoxymethylene)triphenylphosphorane in xylene at reflux resulted in isolation of the corresponding 5,10- and 5,15-bis-β-(ethoxycarbonyl)vinyl derivatives **11** and **12** in 70% yield. Subsequent treatment (of **11** or **12**) with concentrated sulfuric acid led to rapid demetalation and isolation of the two key intermediates 5,10-bis[β-(ethoxycarbonyl)vinyl]octaethylporphyrin (**6**) and 5,15 bis[β-(ethoxycarbonyl)vinyl]octaethylporphyrin (**7**) (90% yield each).

Cyclization of the 5,15-isomer **7** was performed in glacial acetic acid at reflux under nitrogen (Scheme II). The reaction was monitored by visible spectroscopy (aliquots

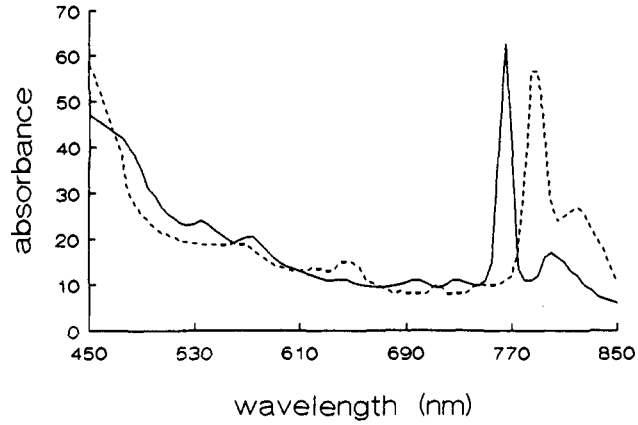

Figure 3. Visible absorption spectra of bispurpurins **13a** (solid line) and **13b** (dashed line).

were periodically taken from the reaction mixture, neutralized with aqueous sodium bicarbonate, and extracted into methylene chloride) specifically monitoring the region between 550 and 600 nm for a strong absorption indicative of isobacteriochlorin formation through cyclizations to *adjacent* pyrrole rings and the region near 750 nm for the characteristic absorption of bacteriochlorins formed through cyclization to *opposite* pyrrole rings. Within 2 h of reflux, an absorption band, which continued to grow over a period of 6 days, was observed at 763 nm. At no time during this period were absorptions characteristic of isobacteriochlorin **14** evident leading to the conclusion that not only does cyclization of both *meso*-β-(ethoxycarbonyl)vinyl groups (of **7**) occur, but also that the reaction is regiospecific, giving the bacteriochlorin **13a**.

Unfortunately, additional spectroscopic evidence to support our conclusions could not be obtained since the product of the reaction proved to be air-sensitive. Exposure of a solution of the bacteriochlorin **13a** in dichloromethane to air resulted in complete photobleaching within a 4-h period. However, additional evidence for bacteriochlorin formation was given when nickel acetate was added to the reaction mixture and reflux continued for a further 24 h. Once again the product of the reaction (the nickel bacteriochlorin **13b**) proved to be air-sensitive with photobleaching causing complete destruction of the bacteriochlorin chromophore within 2 h to exposure to air. However, the visible spectrum of the nickel complex **13b** gave a large absorption band at 775 nm, i.e. red-shifted by 12 nm from the metal-free parent macrocycle **13a** (Figure 3). This observed red-shift is also seen on incorporation of magnesium into bacteriopheophorbide and is contrasted to the blue-shift observed on incorporation of metals into porphyrins, chlorins, or isobacteriochlorins.[1,11]

As expected from the above observations, attempts to cyclize the 5,10-isomer **6** gave similar results. Thus, an absorption band at 761 nm confirmed formation of the bacteriochlorin **15** while absence of absorbances ca. 560 nm confirmed the regiospecificity of the reaction. Once again, facile photobleaching of the macrocycle prevented further characterization of the product. In conclusion, therefore, although cyclization of *meso*-bis[β-(ethoxycarbonyl)-vinyl]octaethylporphyrins **6** and **7** appears to be a viable process, the ease of aerial oxidation of the resulting bacteriochlorins would appear to preclude their use as photosensitizers for photodynamic therapy.

From 2-Oxo-12,13-dihydroxy-3,3,7,8,12,13,17,18-octaethylporphyrin (Diels–Alder Route). As demonstrated

(9) Nichol, A. W. *J. Chem. Soc. C* **1970**, 903.
(10) Smith, K. M.; Bisset, G. M. F.; Cas, K. S.; Tabba, J. D. *Tetrahedron Lett.* **1980**, *21*, 3747.
(11) Chang, C. K. *Biochemistry* **1980**, *19*, 1971.

Scheme II. Attempted Cyclization of Bisacrylates **6** and **7**[a]

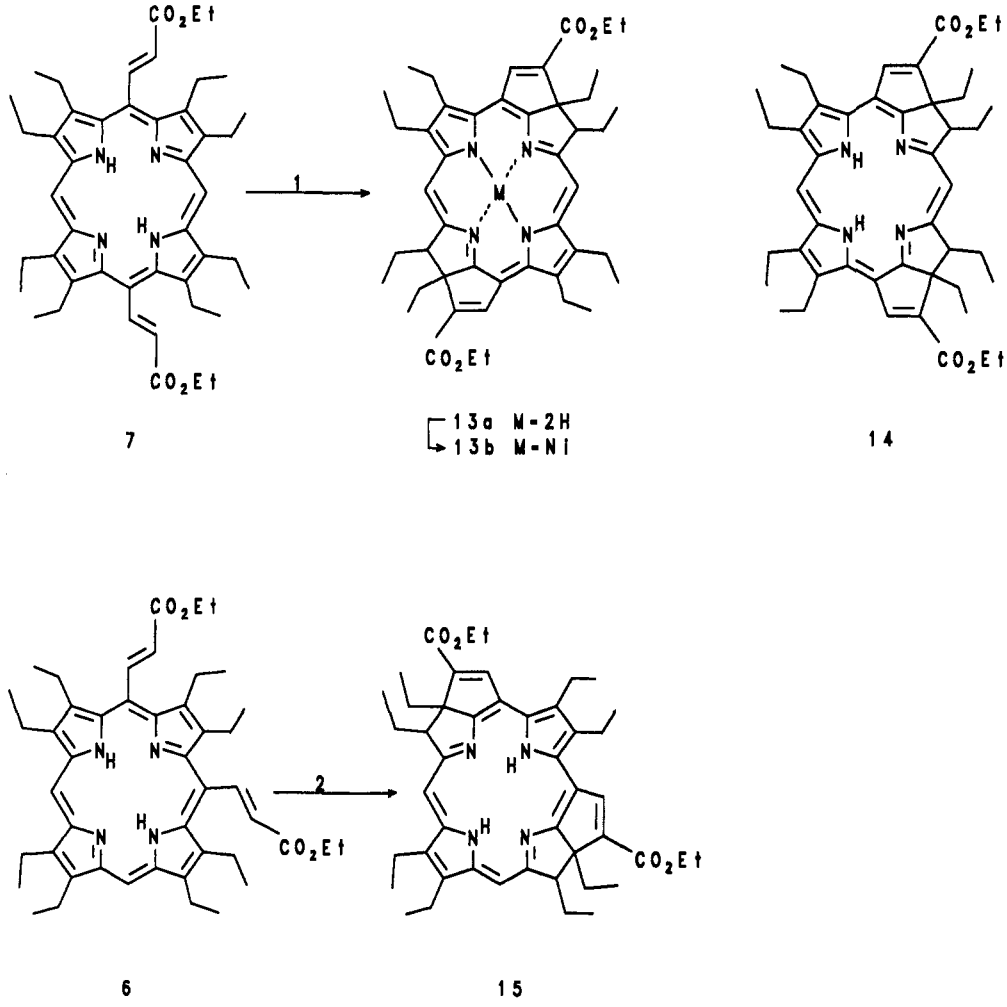

[a] (1 = 2) $HOAc/N_2$.

by our above observations, the preparation of stable bacteriochlorin systems remains a synthetic challenge. One possible route which has previously been described involves the preparation[12] of porphyrindiones (e.g. **16a**), a class of bacteriochlorin that absorbs maximally in the visible spectrum at 700 nm. Reactions of such diones have been shown to generate other bacteriochlorins with absorptions red-shifted by up to 40 nm (**16a** → **17a**, **18a**; Scheme III).[13] All these compounds appear to be more resistant toward oxidation than are other bacteriochlorin systems and are thus perhaps better suited for PDT. We have in fact recently described the in vivo photodynamic activity of some derivatives (**16b**, **17b**, **18b**) against the FANFT-induced urothelial tumor, transplanted into rats.[7c]

During the course of those studies, dione **16b** was generated by pinacol rearrangement of diol **19b**. We reasoned that changing reaction conditions to generate a conjugated diene system (e.g. **20b**) would allow modification of the ring via a Diels–Alder reaction, a method we have previously used to generate a series of adducts that were shown to be active photodynamic agents in vivo.[7b] In the present study it was of interest to determine the effect of cycloaddition on the visible spectrum of **19b** and also to determine the photodynamic efficiencies of the resulting molecules.

Unfortunately, although transformations of porphyrin glycols to the corresponding vinyl derivatives have been reported previously,[7b,14] treatment of **19b** either with acid or in vacuo at temperatures from 135 to 150 °C produced only complex mixtures that could not be further purified.

Better results were obtained, however, with the corresponding diol obtained from octaethylporphyrin (i.e. **19a**). Thus, diol **19a** was converted into the vinyl derivatives **20a/21** by treatment with hydrochloric acid. That dehydration rather than rearrangement had occurred was evident from the ^1H NMR spectrum of the product, which contained resonances (doublet of doublets at δ 8.12, 6.22, 6.07 ppm) attributable to the vinyl moieties (of **20a/21**). In addition, the presence of four signals attributable to the meso protons at C-15 and C-20 (in equal ratios) indicated that both 17-vinyl and 18-vinyl isomers **20a/21** had been formed in equal yields. All attempts at separation were unsuccessful, and so all subsequent cycloadditions were performed on this mixture.

Reaction (of **20a/21**) with TCNE resulted in a high yield (89%) of the corresponding [4 + 2] adducts **22/23** (Scheme IV). Again, attempts to separate each isomer were unsuccessful; however, the mixture was characterized by ^1H NMR spectroscopy, in particular by the presence of resonances for the ethyl group attached to the reduced pyrrole ring and for the protons of the newly formed exocyclic ring (see experimental). Mass spectrometry, using the direct

(12) Inhoffen, H. H.; Nolte, W. *Justus Liebigs Ann. Chem.* **1969**, *725*, 167.
(13) Chang, C. K.; Young, R.; Barkigia, K. M.; Fajer, J. *J. Am. Chem. Soc.* **1984**, *106*, 6457.
(14) Chang, C. K.; Sotiriou, C. *J. Org. Chem.* **1987**, *52*, 926.

Scheme III. Synthesis of Porphyrinone Derivatives[a]

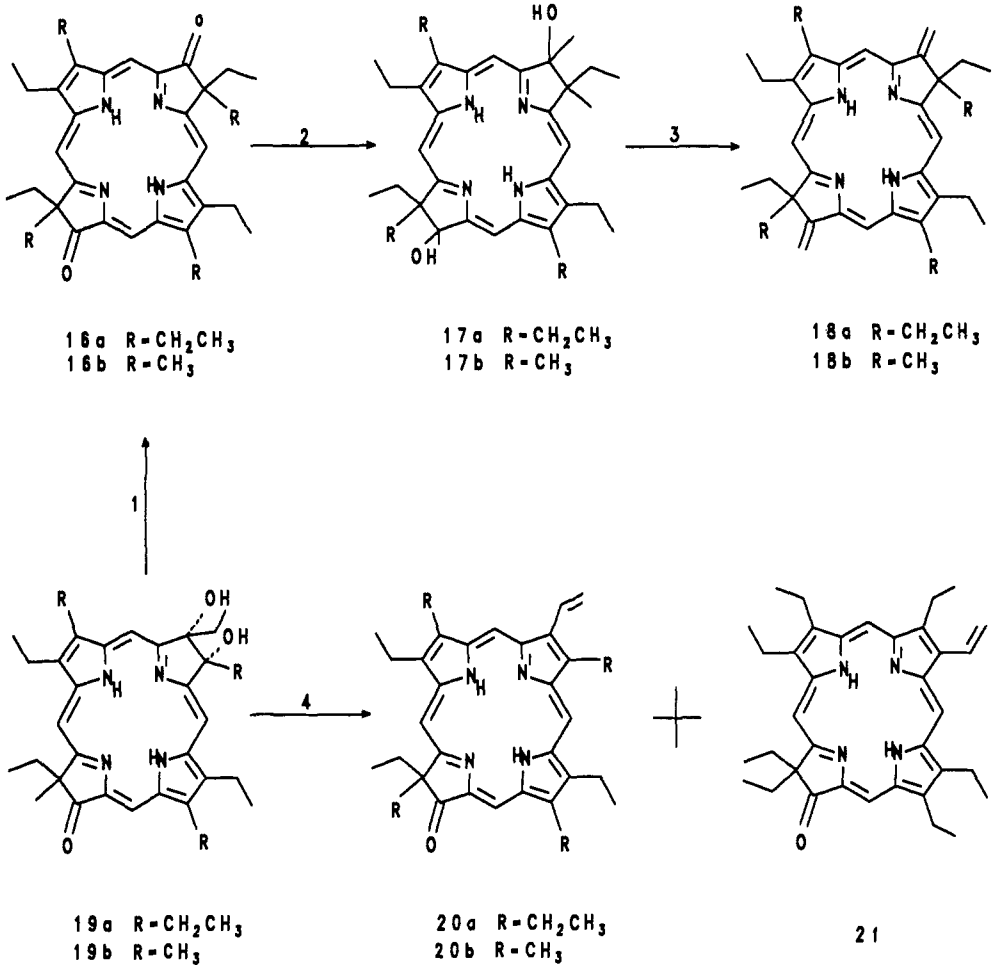

[a] (1) $HClO_4$; (2) MeLi/H^+; (3) H^+; (4) H^+.

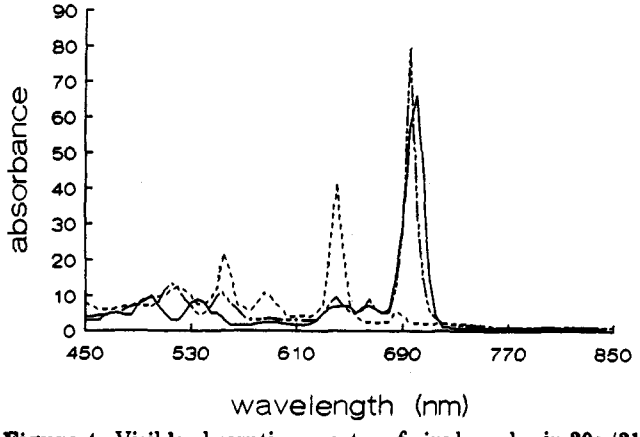

Figure 4. Visible absorption spectra of vinylporphyrin **20a/21** (dotted line) and Diels–Alder adducts **22/23** (solid line) and **24/25** (dashed line).

insertion probe method (DIP), failed to detect the parent ion, presumably due to a retro-Diels–Alder reaction occurring on the heated probe; however, fast atom bombardment techniques (FAB) were successful.

In a similar manner, treatment of **20a/21** with DMAD led to a 46% yield of the corresponding adducts **24/25** following 4 days of reflux in toluene.

The visible spectra of Diels–Alder adducts **22/23** and **24/25** are shown in Figure 4 and compared to that of the vinyl precursor **20a/21**. As expected, formation of bacteriochlorin chromophor results in an increase in intensity of the Q band; however, the wavelength of absorption

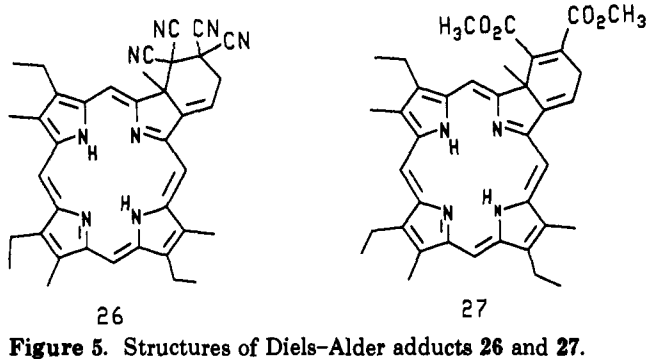

Figure 5. Structures of Diels–Alder adducts **26** and **27**.

resembles that of the porphyrindiones and derivatives rather than that of bacteriochlorophylls.

Despite this, the goal of preparing stable bacteriochlorin systems with absorptions more intense and more red-shifted than that of Photofrin II was achieved and the next phase of this study was initiated.

In Vivo Studies. Bacteriochlorins **13a**, **13b**, and **15** proved to be too air-sensitive to allow in vivo testing; however, **22/23** and **24/25** (each used as a 50:50 mixture of isomers) were stable and therefore examined further. In addition, vinyl derivatives **20a/21** was also tested to allow a comparison of the activity of all three photosensitizers against the reported activity of Diels–Alder adducts **26** and **27** (Figure 5).

Figure 6 shows the effect of each sensitizer on the FANFT-induced urothelial cell carcinoma transplanted into the flanks of Fisher CDF (F344/CrlBr) rats. The

Scheme IV. Diels–Alder Adducts of Vinylporphyrinones **20a/21**[a]

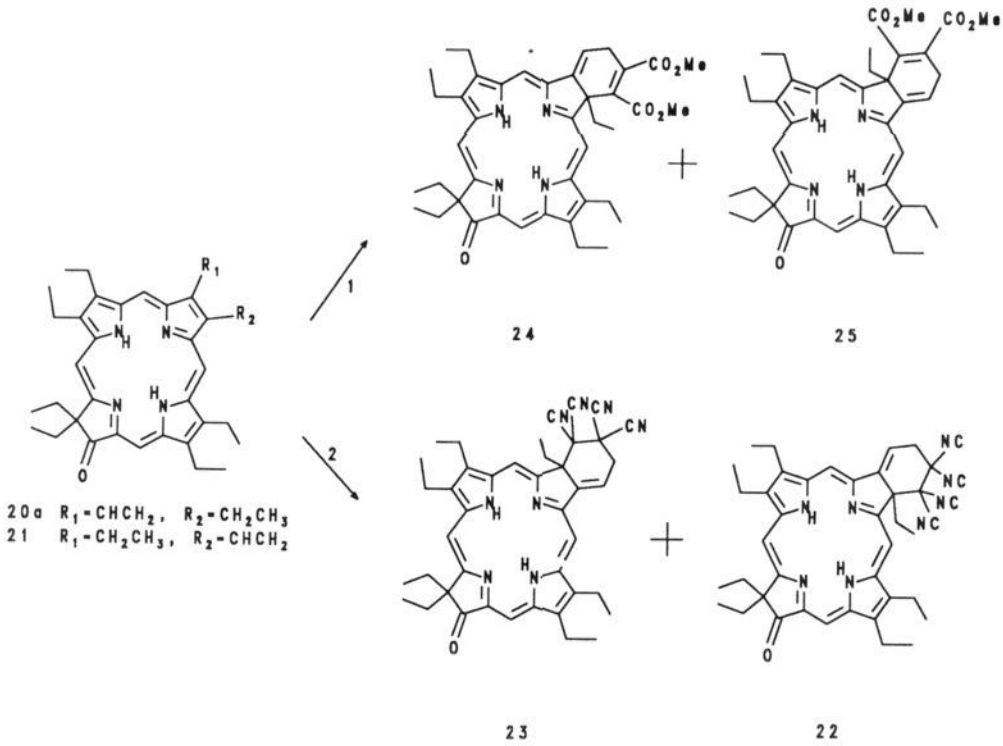

[a] (1) DMAD/toluene; (2) TCNE/$CHCl_3$.

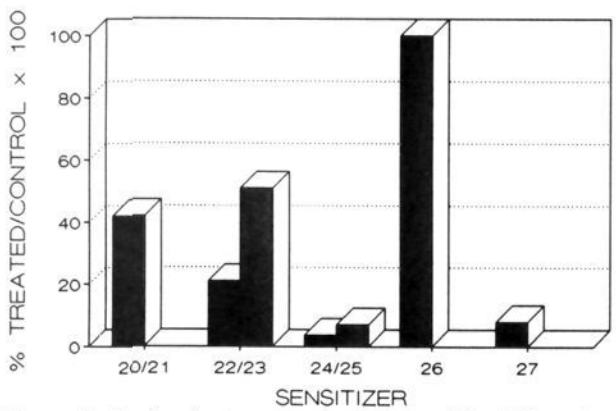

Figure 6. Twelve-day tumor response, dry weight 12 days after phototherapy. For each sensitizer are given dose (mg/kg):statistical significance (NS = not statistical):animals free of palpable tumor. **20/21** (2.5:$p < 0.05$:20%); **22/23** (filled box, 2.5:NS:50%; patterned box, 1.0:NS:0%); **24/25** (filled box, 1.0:$p < 0.04$:75%; patterned box, 0.5:$p < 0.01$:20%); **26** (1.0:NS:0%); **27** (1.0:$p < 0.006$:50%).

results are expressed as dry tumor weight of treated tumors as a percentage of control tumors, 12 days following phototherapy.

As can be seen, TCNE adducts **22/23** showed some activity in this tumor model with 50% of animals free of palpable tumor, following irradiation of a 2.5 mg/kg dose; however, activity quickly decreased on reduction of the sensitizer dose to 1 mg/kg, consistent with our previously reported data for TCNE adduct **26**. Conversely, DMAD adduct **24/25** proved to be a very efficient photodynamic agent, with 75% animals treated with a dose of 1 mg/kg body weight free of palpable tumor 12 days after irradiation. Again, this result is consistent with the high activity previously described for DMAD adduct **27**.[7b] Lowering the dose of **24/25** to 0.5 mg/kg resulted in a decrease in activity as expected, although 20% of animals were still free of palpable tumor on day 12 post therapy. Finally, the vinyl derivative **20a/21** was the least effective of all with a dose of 2.5 mg/kg needed to cause significant tumor regression (20% animals free of palpable tumor).

In conclusion, the technique of increasing the wavelength of absorption bands into the red region of the visible spectrum while retaining in vivo activity is desirable since longer red-absorbing sensitizers may show beter photodynamic action in larger tumors (due to the increased penetration of light through tissues at these wavelengths[15]). In the present study we have shown that introduction of a keto group into a previously determined photodynamically active agent (**27**) leads not only to a red-shift in absorption by ca. 40 nm but also to a new sensitizer, which, under our protocol, appears to be at least as active in vivo. Further comparative studies using **22/23** and **24/25** are in progress to determine the effect of introduction of a keto group on other parameters important for photodynamic therapy, including tissue distribution and retention, depth of necrosis following irradiation, and photophysical properties.

Experimental Studies

Visible spectra were recorded on a Bauch and Lomb Spectronic 2000; absorptions are given in nanometers (solutions in dichloromethane). Proton nuclear magnetic resonance spectra (^1H NMR) were obtained on a JEOL FX-90Q or a Varian VXR400 spectrometer; chemical shifts are expressed in parts per million downfield from internal tetramethylsilane. Low-resolution mass spectra were measured (direct insertion probe) on a Hewlett-Packard 5987 mass spectrometer or (fast atom bombardment) on a JEOL HX110 mass spectrometer located at the Michigan State Mass Spectrometry Center. Analytical TLC was performed by using Merck silica gel 60F 254 precoated sheets (0.2 mm);

(15) Wan, S.; Parrish, J. A.; Anderson, R. R.; Madden, M. *Photochem. Photobiol.* **1981**, *34*, 679.

preparative chromatography was performed on a Chromatotron, using Merck silica gel 60F 254 with $CaSO_4$-$^1/_2H_2O$. Elemental analyses were performed by MicAnal, Tucson, AZ 85717.

Nickel 5-[β-(Ethoxycarbonyl)vinyl]-10-formyloctaethylporphyrin (9) and Nickel 5-[β-(Ethoxycarbonyl)vinyl]-15-formyloctaethylporphyrin (10). A 14-mL portion of Vilsmier reagent, prepared by dropwise addition of $POCl_3$ (9 mL) to DMF (5 mL) at 0 °C and allowing the resulting solution to stand at room temperature for 0.5 h was added to 1,2-dichloroethane (12 mL) and warmed on a water bath to 60–65 °C. To this solution was added dropwise with stirring a solution of nickel *meso*-[β-(ethoxycarbonyl)vinyl]octaethylporphyrin (8) (300 mg) in dry 1,2-dichloroethane (120 mL). The reaction mixture was stirred for an additional hour while the temperature was maintained at 60–65 °C. A saturated solution of sodium acetate (225 mL) was then added, and stirring and heating were continued for 2 more hours. The organic phase was separated and washed with water three times, and the solvent was removed under reduced pressure. The resulting solid was chromatographed on silica gel using dichloromethane as eluent. Two bands were collected. Each was evaporated to dryness and recrystallized from methanol–dichloromethane (80:20).

Fraction 1 (85 mg, 27%), nickel 5-[β-(ethoxycarbonyl)vinyl]-10-formyloctaethylporphyrin (9): ^{1}H NMR ($CDCl_3$) δ 11.59 (s, 1 H, C*H*O), 9.77 (d, 1 H, *J* = 15 Hz, PC*H*=CH), 9.07, 9.01 (s, 1 H each, meso H), 5.35 (d, *J* = 15 Hz, 1 H, PCH=C*H*), 4.27 (q, 2 H, $CO_2CH_2CH_3$), 3.61 (m, 16 H, CH_2CH_3), 1.61 (m, 24 H, CH_2CH_3), 1.30 (t, 3 H, $CO_2CH_2CH_3$); mass spectrum calcd *m/e* 716, found (FAB) 717 (M + 1); λ_{max} 410, 575 (sh), 652 nm (ε 90231, 6659, 8071). Anal. Calcd for $C_{42}H_{50}N_4NiO_3$: C, 70.39; H, 7.11; N, 7.81. Found: C, 70.8; H, 7.09; N, 7.57.

Fraction 2 (42 mg, 14%), nickel 5-[β-(ethoxycarbonyl)vinyl]-15-formyloctaethylporphyrin (10): ^{1}H NMR ($CDCl_3$) δ 11.64 (s, 1 H, C*H*O), 9.77 (d, *J* = 15 Hz, 1 H, PC*H*=CH), 9.07 (s, 2 H, meso H), 5.33 (d, 1 H, *J* = 15 Hz, PCH=C*H*), 4.27 (q, 2 H, $CO_2CH_2CH_3$), 3.60 (m, 16 H, CH_2CH_3), 1.60 (m, 24 H, CH_2CH_3), 1.30 (t, 3 H, $CO_2CH_2CH_3$); mass spectrum calcd *m/e* 716, found (FAB) 717 (M + 1); λ_{max} 422, 575 (sh), 655 (ε 91110, 4480, 7348). Anal. Calcd for $C_{42}H_{50}N_4NiO_3$: C, 70.39; H, 7.11; N, 7.81. Found: C, 70.16; H, 7.04; N, 7.30.

Nickel 5,10-Bis[β-(ethoxycarbonyl)vinyl]octaethylporphyrin (11). A solution of **9** (50 mg) and (carbethoxymethylene)triphenylphosphorane (300 mg) in xylene (50 mL) was heated under reflux for 24 h. The resulting solution was cooled, and the solvent was removed under reduced pressure. Chromatography of the crude product on silica with dichloromethane containing 25% hexane as eluent gave a major band, which was collected. Removal of the solvent and crystallization of the residue using methanol–dichloromethane (80:20) gave the product 11 (40 mg, 71%): ^{1}H NMR ($CDCl_3$) δ 9.86 (d, *J* = 16 Hz, 1 H, 2 PC*H*=CH), 9.15 (s, 2 H, meso H), 5.16 (d, 1 H, *J* = 16 Hz, 2 PCH=C*H*), 4.25 (q, 4 H, $CO_2CH_2CH_3$), 3.67 (m, 16 H, CH_2CH_3), 1.75, 1.70 1.62, 1.55 (all t, 24 H, CH_2CH_3), 1.31 (t, 6 H, $CO_2CH_2CH_3$); λ_{max} 405, 545 (sh), 580 (ε 105520, 18121, 40134).

Nickel 5,15-Bis[β-(ethoxycarbonyl)vinyl]octaethylporphyrin (12). The metalloporphyrin **10** (50 mg) was treated with carbethoxymethylene)triphenylphosphorane (300 mg) as described above to give 38 mg (67%) of the product **13**: ^{1}H NMR ($CDCl_3$) δ 9.87 (d, 1 H, *J* = 16 Hz, 2 PC*H*=CH), 9.18 (s, 2 H, meso H), 5.22 (d, 1 H, *J* = 16 Hz, 2 PCH=C*H*), 4.24 (q, 4 H, $CO_2CH_2CH_3$), 3.64 (m, 16 H, CH_2CH_3), 1.70, 1.65 (both t, 24 H, CH_2CH_3), 1.29 (t, 6 H, $CO_2CH_2CH_3$); λ_{max} 410, 550 (sh), 577 (ε 108579, 16371, 38572).

5,10-Bis[β-(ethoxycarbonyl)vinyl]octaethylporphyrin (6). A solution of the nickel complex 11 (25 mg) was dissolved in concentrated sulfuric acid (2 mL), and the solution was kept for 2 h at room temperature. Dichloromethane (20 mL) was added followed by saturated aqueous sodium hydrogen carbonate. After neutralization, the organic layer was collected, washed, and dried. The solvent was removed under reduced pressure, and the crude product was recrystallized from methanol–dichloromethane (80:20) to give 21 mg (90%) of the product **6**: ^{1}H NMR ($CDCl_3$) δ 10.15 (d, 1 H, *J* = 15 Hz, 2 PC*H*=CH), 9.54 (s, 2 H, meso H), 6.29 (d, 1 H, *J* = 15 Hz, 2 PCH=C*H*), 4.44 (q, 4 H, $CO_2CH_2CH_3$), 3.85 (m, 16 H, CH_2CH_3), 1.78, 1.72, 1.68 (q, 24 H, CH_2CH_3), 1.46 (t, 6 H, $CO_2CH_2CH_3$), −2.10 (br s, 2 H, N*H*); mass spectrum calcd *m/e* 730, found (DIP) *m/e* 730; λ_{max} 410, 515, 544, 570, 620 (ε 134033, 5002, 2134, 612). Anal. Calcd for $C_{46}H_{58}N_4O_4 \cdot 0.5H_2O$: C, 74.69; H, 7.98; N, 7.57. Found: C, 74.85; H, 7.94; N, 7.25.

5,15-Bis[β-(ethoxycarbonyl)vinyl]octaethylporphyrin (7). The nickel complex 12 (25 mg) was treated with sulfuric acid (2 mL) as described above to give 21 mg (90%) of the product **7**: ^{1}H NMR ($CDCl_3$) δ 10.25 (d, *J* = 15 Hz, 1 H, 2 PC*H*=CH), 10.03 (s, 2 H, meso H), 6.18 (d, *J* = 15 Hz, 1 H, 2 PCH=C*H*), 4.44 (q, 4 H, $CO_2CH_2CH_3$), 4.00 (q, 8 H, CH_2CH_3), 3.85 (q, 8 H, CH_2CH_3), 1.80, 1.65 (t, 24 H, CH_2CH_3), 1.44 (t, 6 H, $CO_2CH_2CH_3$); mass spectrum calcd *m/e* 730, found (DIP) *m/e* 730; λ_{max} 414, 509, 545, 573, 627 (ε 136230, 4675, 2329, 2420, 502). Anal. Calcd for $C_{46}H_{58}N_4O_4 \cdot 0.5H_2O$: C, 74.69; H, 7.98; 7.57. Found: C, 74.88; H, 8.15; N, 7.23.

Attempted Cyclization of 5,15-Bis[β-(ethoxycarbonyl)vinyl]octaethylporphyrin (7). A solution of 5,15-bis[β-(ethoxycarbonyl)vinyl]octaethylporphyrin (7) (30 mg) in glacial acetic acid (20 mL) was refluxed under a nitrogen atmosphere for 6 days. The mixture was monitored by removing a small sample, neutralizing with sodium bicarbonate, extracting the product into dichloromethane, and recording the visible spectrum. Reaction was determined to be complete by following the increase with time of an absorption band at 763 nm (attributed to formation of **13a**) to its maximum. At this time the reaction mixture was allowed to cool and the solvent was removed under reduced pressure. The resulting black solid was extracted with dichloromethane. Spectra of this sample were recorded periodically and showed a progressive decline in the intensity of the 763-nm band (which disappeared after 4 h).

Repeating the reaction in propionic acid led to similar observations, except that reaction appeared to be complete in 4 days.

Attempted Preparation of the Nickel Complex of Bacteriochlorin 13. A solution of **7** (30 mg) was treated as described above to generate bacteriochlorin **13a**. To the resulting solution was added nickel acetate (30 mg), and reflux was continued for 4 additional hours. The visible spectrum of the cooled solution (after neutralization and dilution with dichloromethane) showed an intense absorption band at 775 nm (**13b**). Removal of the solvent under reduced pressure left a black solid that was extracted with dichloromethane. The visible spectrum of this solution was recorded over a 2-h period when a progressive decrease in the intensity of the 775-nm band was observed.

Attempted Cyclization of 5,10-Bis[β-(ethoxycarbonyl)vinyl]octaethylporphyrin (6). Attempts to cyclize the 5,10-bis[β-ethoxycarbonyl)vinyl]octaethylporphyrin (**6**) were carried out as described above for **7**. Similar observations were made.

2-Oxo-12-vinyl-3,3,7,8,13,17,18-heptaethylchlorin (20a) and 2-Oxo-13-vinyl-3,3,7,8,12,17,18-heptaethylchlorin (21). A solution of bacteriochlorin **19** (100 mg) in benzene (50 mL), containing 5 drops of concentrated hydrochloric acid, was refluxed for 3 h. The solvent was evaporated on a rotary evaporator, and the residue was recrystallized using methanol–dichloromethane (80:20), yielding 90 mg (96%) of products **20a** and **21**: ^{1}H NMR ($CDCl_3$) δ 10.08, 9.88 (both s, 1 H each, meso H of one isomer), 10.01, 9.96 (both s, 1 H each, meso H of second isomer), 9.81, 9.11 (both s, 2 H each, meso H*), 8.12 (dd, 2 H, C*H*=CH_2, J_1 = 11.4 Hz, J_2 = 17.8 Hz*), 6.22 (dd, 2 H, CH=CH_2, J_1 = 1.6 Hz, J_2 = 17.8 Hz*), 6.07 (dd, 2 H, CH=CH_2, J_1 = 1.6 Hz, J_2 = 11.6 Hz*), 4.05 (m, 20 H, CH_2CH_3*), 2.77 (q, 8 H, geminal CH_2CH_3*), 1.85 (m, 30 H, CH_2CH_3*), 0.38 (t, 12 H, geminal CH_2CH_3*), −2.86 (br s, 2 H, N*H* of one isomer), −2.85 (br s, 2 H, N*H* of the other isomer) [* resonances for both isomers]; mass spectrum calcd *m/e* 548, found (DIP) *m/e* 548; λ_{max} 407, 513, 554, 584, 640, 686 (ε 155958, 12513, 20002, 10503, 39182, 6119). Anal. Calcd for $C_{36}H_{44}N_4O \cdot 3H_2O$: C, 71.76; H, 8.30; N, 8.33. Found: C, 71.98; H, 8.01; N, 8.33.

Diels–Alder Additions to Oxovinylheptaethylchlorin Isomers (20a, 21). TCNE Adducts (22/23). TCNE (20 mg) was added to the mixture of ketovinylheptaethylcholin **20a/21** (20 mg) in chloroform (25 mL), and the resulting solution was refluxed for 2 h. After cooling, the solvent was evaporated and the residue was recrystallized from dichloromethane–hexane (20:80) to yield 22 mg (89%) of adduct **22/23**: ^{1}H NMR ($CDCl_3$) δ 9.65, 9.63, 9.34, 9.28, 9.20, 9.08, 8.94, 8.87 (all s, 1 H each, 8 meso H, four for each isomer), 7.20 (m, 2 H, C=C*H**), 4.10 (m, 4 H, $CHCH_2$*), 3.90 (m, 16 H, CH_2CH_3*), 2.90 (q, 4 H, CH_2 of sp^3

ethyl*), 2.65 (m, 8 H, geminal CH_2CH_3*), 1.95 (m, 24 H, CH_2CH_3*), 0.45, 0.35 (t, 6 H each, geminal CH_2CH_3*), 0.25 (t, 6 H, CH_3 of sp^3 ethyl*), -2.25, -2.20, -2.15, -2.10 (all s, 1 H each, NH, two for each isomer) [*resonances for both isomers]; high-resolution mass spectrum calcd for $C_{42}H_{44}N_8O$ m/e 676.3668, found m/e 676.3669; λ_{max} 416, 504, 543, 634, 665, 698 (ϵ 110729, 11540, 9673, 8654, 7976, 59395).

DMAD Adducts (24/25). A mixture of the two ketovinylheptaethylchlorin isomers **20a/21** (50 mg) in toluene (50 mL) was treated with DMAD (5 mL), and the resulting solution was refluxed for 4 days. The solution was cooled, the solvent was removed under reduced pressure, and the residue was chromatographed on silica gel using dichloromethane containing 2% ether and 2% toluene as eluent.

The first (red) band was collected, the solvent was removed, and the residue was recrystallized from methanol-dichloromethane (80:20) to give recovered reactants **20a/21**, 12 mg (24%).

The second (brown) band was worked up as described above to give the expected Diels-Alder isomers **24/25** in 23% yield: ^1H NMR ($CDCl_3$) δ 9.54, 9.23, 9.10, 8.92, 8.81, 8.71 (all s, 1 H each, 8 meso H), 7.32 (dd, 1 H, C=CH*), 3.95-3.80 (m, $CHCH_2$, CH_2CH_3*), 3.95 (s, 3 H, CO_2CH_3*), 3.87 (s, 3 H, CO_2CH_3*), 2.60 (q, 4 H, geminal CH_2CH_3*), 2.58 (m, 2 H, diastereotropic CH_2 of sp^3 ethyl*), 1.76 (m, 12 H, CH_2CH_3*), 0.41, 0.37, 0.33 (all t, 9 H, CH_2CH_3 of reduced pyrroles*), -2.35, -2.30 (both s, 2 H, NH*) [*resonances for both isomers[; high-resolution mass spectrum calcd for $C_{42}H_{50}N_4O_5$ m/e 690.3750, found m/e 690.3749; λ_{max} 400, 420, 504, 543, 649, 669, 707 (ϵ 98744, 135764, 8603, 8016, 6257, 6713, 56052).

Tumor Model. The tumor model has been fully described.[22] The FANFT-induced rat bladder tumor (AY-27) was implanted subcutaneously into the flanks of Fischer CDF (F344/ClBr) rats. When tumors were 1 cm in transverse diameter (after 10 days), animals (n = 5) were injected IV with sensitizer previously emulsified using Cremophor EL. Twenty-four hours later, one tumor was shielded (serving as an internal control) and the second tumor irradiated with red light from a Kodak slide projector fitted with a sharp cut filter at 590 nm. Power density was 200 mW/cm^2 and irradiation time 30 min (total energy delivered = 360 J/cm^2). Intratumor temperature was monitored with a thermistor probe and was found to raise by no more than 1 °C above body temperature. Following irradiation, animals were kept for 12 days, sacrificed, and control and treated tumors excised. Tumors were freed of surrounding tissue and subcutaneous tissue and desiccated to constant weight.

Acknowledgment. This work was supported in part by Grants CA 43006 and CA 48733 from the National Cancer Institute, NIH, DHHS. We also wish to thank the Michigan State Mass Spectrometry Facility, supported in part by NIH Grant No. DRR-00480 for fast atom bombardment measurements and high-resolution mass spectra.

Functionalized Congener Approach to Muscarinic Antagonists: Analogues of Pirenzepine

Yishai Karton,[†,‡] Barton J. Bradbury,[†] Jesse Baumgold,[§] Robert Paek,[§] and Kenneth A. Jacobson*[,†]

Laboratory of Bioorganic Chemistry, NIDDK, National Institutes of Health, Bethesda, Maryland 20892, and Department of Radiology, George Washington University, Washington, D.C. 20037. *Received October 17, 1990*

The M_1-selective muscarinic receptor antagonist pirenzepine (5,11-dihydro-11-[(4-methyl-1-piperazinyl)acetyl]-6*H*-pyrido[2,3-*b*][1,4]benzodiazepin-6-one) was derivatized to explore points of attachment of functionalized side chains for the synthesis of receptor probes and ligands for affinity chromatography. The analogues prepared were evaluated in competitive binding assays versus [^{3}H]-*N*-methylscopolamine at four muscarinic receptor subtypes (m1AChR-m4AChR) in membranes from rat heart tissue and transfected A9L cells. 9-(Hydroxymethyl)pirenzepine, 8-(methylthio)pirenzepine, and a series of 8-aminosulfonyl derivatives were synthesized. Several 5-substituted analogues of pirenzepine also were prepared. An alternate series of analogues substituted on the 4-position of the piperazine ring was prepared by reaction of 4-desmethylpirenzepine with various electrophiles. An *N*-chloroethyl analogue of pirenzepine was shown to form a reactive aziridine species in aqueous buffer yet failed to affinity label muscarinic receptors. Within a series of aminoalkyl analogues, the affinity increased as the length of the alkyl chain increased. Shorter chain analogues were generally much less potent than pirenzepine, and longer analogues (7-10 carbons) were roughly as potent as pirenzepine at m1 receptors, but were nonselective. Depending on the methylene chain length, acylation or alkyl substitution of the terminal amine also influenced the affinity at muscarinic receptors.

Muscarinic cholinergic receptors (mAChRs) mediate the actions of the neurotransmitter acetylcholine in the central and peripheral nervous systems,[1] gastrointestinal system,[2] heart,[3] endocrine glands,[4] lungs,[5] and other tissues. At least five distinct gene products[6-8] have been identified that code for five distinct mAChRs, termed m1 through m5. The m1, m2, and m3 receptors correlate pharmacologically to the M_1, M_2, and M_3 (M_2 glandular) receptors, respectively.[9] The m1 and m3 receptors have been shown to be coupled preferentially to the stimulation of phosphoinositide metabolism,[7] and m2 and m4 receptors have been shown to be coupled preferentially to the inhibition of adenylate cyclase.[7,10] Other effector systems such as voltage-dependent[11] and calcium-dependent[12] potassium channels are

* Author to whom correspondence should be addressed at Bldg. 8A, B1A-17, National Institutes of Health, Bethesda, MD 20892.
† National Institutes of Health.
‡ On leave from the Israel Institute for Biological Research, Nes Ziona, Israel.
§ George Washington University.

(1) *Central Cholinergic Synaptic Transmission*; Frotscher, M., Misgeld, U., Eds.; Birkhauser Verlag: Basel, 1989.
(2) Kromer, W.; Gönne, S. *Int. J. Exp. Clin. Pharmacol.* **1988**, *37* (suppl. 1), 48.
(3) (a) Melchiorre, C.; Cassinelli, A.; Quaglia, W. *J. Med. Chem.* **1987**, *30*, 201. (b) Melchiorre, C.; Cassinelli, A.; Angeli, P.; Giardina, D.; Gulini, U.; Quaglia, W. *Trends Pharm. Sci.* (supplement) **1988**, 55.
(4) Goyal, R. *New Engl. J. Med.* **1989**, *321*, 1022.
(5) Maclagan, J.; Barnes, P. *Trends Phar. Sci.* **1989** (Suppl. "Subtypes of Muscarinic Receptors IV"), 88-92.
(6) (a) Bonner, T. I.; Buckley, N. J.; Young, A. C.; Brann, M. R. *Science* **1987**, *237*, 527. (b) Bonner, T. I.; Young, A. C.; Brann, M. R.; Buckley, N. J. *Neuron* **1988**, *1*, 403.
(7) Peralta, E. G.; Ashkenazi, A.; Winslow, J. W.; Ramachandran, J.; Capon, D. J. *Nature* **1988**, *334*, 434.
(8) Maeda, A.; Kubo, T.; Mishina, M.; Numa, S. *FEBS Lett.* **1988**, *239*, 339.